Multi-Touch Skin: A Thin and Flexible Multi-Touch Sensor for On-Skin Input

Aditya Shekhar Nittala*   **Anusha Withana***   **Narjes Pourjafarian**   **Jürgen Steimle**

Saarland University, Saarland Informatics Campus, Germany

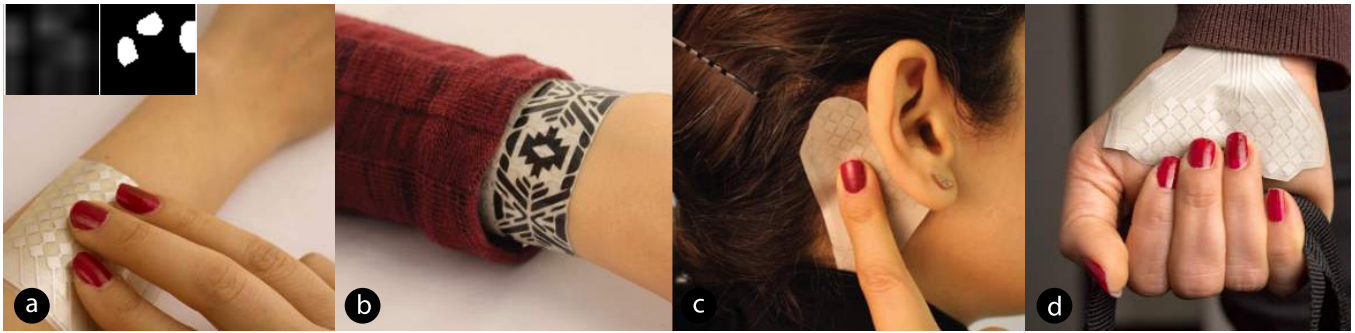{nittala, anusha, steimle}@cs.uni-saarland.de, s8napour@stud.uni-saarland.de

Figure 1. The thin and flexible multi-touch sensor can be customized in size and shape to fit various locations on the body: a) multi-touch input on the forearm for remote communication (inset shows capacitive image); b) multi-touch-enabled bracelet with an art-layer for aesthetic customization; c) input behind the ear; d) input on the palm with busy hands.

ABSTRACT

Skin-based touch input opens up new opportunities for direct, subtle, and expressive interaction. However, existing skin-worn sensors are restricted to single-touch input and limited by a low resolution. We present the first skin overlay that can capture high-resolution multi-touch input. Our main contributions are: 1) Based on an exploration of functional materials, we present a fabrication approach for printing thin and flexible multi-touch sensors for on-skin interactions. 2) We present the first non-rectangular multi-touch sensor overlay for use on skin and introduce a design tool that generates such sensors in custom shapes and sizes. 3) To validate the feasibility and versatility of our approach, we present four application examples and empirical results from two technical evaluations. They confirm that the sensor achieves a high signal-to-noise ratio on the body under various grounding conditions and has a high spatial accuracy even when subjected to strong deformations.

ACM Classification Keywords

H.5.2. User Interfaces: Input devices and strategies.

Author Keywords

Fabrication; On-body input; Multi-touch input; Wearable computing; Flexible sensor; Electronic skin.

*The first two authors contributed equally to this work.

INTRODUCTION

The human body offers a large and quickly accessible surface for always-available, eyes-free interaction [16]. For these reasons, sensing touch input on the body has received considerable attention in the HCI community. Various technical approaches have been presented, including computer vision [17], magnetic [6, 22], bio-acoustic and electro-magnetic wave propagation [19, 37, 55], and capacitive sensing [24, 32, 52, 54]. However, empirical studies show that our body affords a wider variety of touch-based interactions [53]. These interactions require high-resolution multi-touch input, which is beyond the capabilities of state-of-the-art touch sensors for the body.

The industry standard for high-resolution multi-touch input is mutual-capacitance sensing [3]. Such sensors are commonplace inside objects and mobile devices. However, deploying such sensors on the human body poses several challenges: First, the human body surface is curved and deformable; hence the sensor must be very slim and flexible to conform to human skin. Second, the human body has its own electro-capacitive effects, which have to be properly shielded from the body-worn sensor to acquire reliable touch input. Lastly, input locations on the body vary in their size and have various (non-rectangular) shapes; hence, the sensor should support personalization and customization.

In this paper, we introduce Multi-Touch Skin, the first high-resolution multi-touch sensor for on-body interaction. Multi-Touch Skin is thin and flexible to conform to the user's skin. In contrast to prior skin-based touch sensors that used self-capacitance [54, 24, 32], our sensor leverages on mutual-capacitance matrix sensing tailored for the body. This enables scalability and multi-touch input. Furthermore, it can be cus-

tomized to diverse body geometries and is immune to body capacitance effects. More specifically, our contributions are:

We present a *fabrication approach* for realizing Multi-Touch Skin sensors with printed electronics in a simple lab setting. Based on a systematic exploration of functional inks and substrate materials, we introduce the first solution to print a high-resolution multi-touch sensor with a desktop inkjet printer. We also show how to achieve very thin designs using screen printing. Based on the principles from electronic circuit design and previous literature on wearable sensors [1, 14, 35, 48], we present a solution to effectively shield the slim sensor sandwich from stray capacitive noise caused by the electro-capacitive effects of the body, which is a key prerequisite for correct functioning on the body.

Moreover, we contribute a novel approach and design tool to *generate multi-touch sensor designs of custom size and custom shape*. We use these to present the first non-rectangular multi-touch sensor designs for the body.

To validate the feasibility and versatility of the approach, we have realized four *interactive prototypes and application examples*. These highlight new opportunities for on-body interaction and demonstrate that the sensor can be easily customized for use on various body locations. Empirical results from two technical evaluation studies confirm that the sensor achieves a *high signal-to-noise ratio* on the body under various grounding conditions and has a *high spatial accuracy* under different scales and when subject to strong deformation.

Overall, our results demonstrate that high-resolution multi-touch sensors can be realized in very slim and deformable form factors for the body, while offering many customization options for non-conventional sensor shapes.

RELATED WORK
We build upon prior work in the areas of on-body interaction and capacitive touch sensing.

On-Body Interaction
Researchers in the HCI community have been exploring the possibility of appropriating the body as an input surface. Optical approaches have been used to sense input on the body using infrared proximity sensors [26, 38, 40], depth cameras [17, 9] or fish-eye cameras [5]. Other approaches leverage the capability of the human body to propagate sound [19, 37] or electromagnetic waves [55]. Moreover, Hall-effect sensing [6, 22], electric-field sensing [56] and distinct electrical signatures across the human body [34] have been used for localizing on-body gestures. It is also possible to use sonar [29] or radar [30] for sensing finger movements. These approaches are typically restricted to capturing only single-touch input. Another approach is to instrument the body with appropriate sensors for interaction. Wearable systems have been deployed at various body locations which enabled always-available interaction [23, 2, 18]. However, these systems typically use rigid electronics and hence do not adapt to the more complex geometries of the body. Recent advances in printed electronics and electronic skin have enabled thin, flexible, and stretchable skin overlays that can be worn on the body [52]. Slim tattoos

have been used to enable touch and pose sensing along with providing visual output [32, 24, 54, 50], however, are limited to single-touch input.

Capacitive Touch Sensing
Research on capacitive touch screens began in 1970's [4] and grew rapidly, which led to the development of tablets and large touch surfaces [28, 46, 10]. Capacitive touch sensing is also used on a wide variety of physical objects, including metallic objects, water, and even live plants [47, 45]. A recent stream of work is investigating flexible capacitive touch surfaces. For instance, their use has been demonstrated when wrapped around a pen [49], inside textiles [44, 11, 20], and printed on thin paper [41, 12, 33]. There are five commonly used configurations of capacitive sensing to enable touch interaction. A detailed comparison is available in [13]. However, capacitive sensors for touch input on skin have so far been limited to single-capacitance sensing, which prevents the technology from scaling to multi-touch and higher-resolution. Furthermore, while toolkits such as CapSense for Arduino have made single-touch sensing accessible to a wide audience, it remains very difficult to use mutual-capacitance sensing in HCI prototypes. Multi-Touch Skin is based on the mutual-capacitance sensing principle. In contrast to other technologies for on-body touch input, mutual-capacitance sensing enables precise and high-resolution capturing of multiple touch contacts and does not suffer from occlusion problems encountered in optical approaches.

SENSOR FABRICATION
In this section, we present a fabrication approach for realizing thin and flexible multi-touch sensors for use on the body. We start by reviewing the basics of mutual-capacitance touch sensing and contribute a systematic exploration of materials and their combinations that informed our fabrication technique. We present novel fabrication techniques for rapid iterations and for high-fidelity prototyping. This includes the first technique for fabricating a mutual-capacitance multi-touch sensor on a commodity ink-jet printer. The printed sensor readily works with off-the-shelf multi-touch controllers, without requiring fine-tuning of the controller's parameters.

Mutual Capacitance Touch Sensing on Skin
A mutual-capacitance-based touch sensor [3] consists of two overlaid layers of conductors: one with transmit electrodes, and another with receive electrodes. Both layers are electrically insulated from each other by a dielectric material. These electrodes are typically arranged in a 2D row-column matrix pattern creating overlapping intersections, which creates a mutual-capacitance between each transmitter (i.e. row) and receiver (i.e. column) pairs (Figure 2(b)). The transmit layer is driven by a weak alternating current (AC) signal, which is received by the receive electrodes. This received signal can be used to measure changes to the mutual-capacitance between the relevant row and column. When a human finger gets close to one of these intersections, capacitance between the two electrodes is reduced as the electric field between them is disturbed by the finger, which can be detected as a touch down event [57, 13]. Using a time-division multiplexing scheme [3, 10], multiple simultaneous touch points can be detected.

#	Conductor	Dielectric	Substrate	Technique	Functional	Fabrication Speed	Observations
1	Silver	Dielectric Paste	Tattoo Paper	Screen printing	Yes	Slow	Silver and dielectric paste are brittle
2	Carbon	Dielectric Paste	Tattoo Paper	Screen printing	Yes	Slow	Carbon and dielectric paste are brittle
3	PEDOT	Resin Binder	Tattoo Paper	Screen printing	No	Slow	High resistance of PEDOT
4	Silver	PVC film	Tattoo Paper	Screen printing	Yes	Slow	Thin sensor $(70-160\mu m)$; Silver is brittle
5	**Silver+PEDOT**	**PVC film**	**Tattoo Paper**	**Screen printing**	Yes	Slow	Thin sensor $(70-160\mu m)$; PEDOT increases robustness
6	**Silver**	**PVC film**	**PET film**	**Inkjet printing**	Yes	Fast	Prints within a minute; thicker sensor $(\sim 400\mu m)$
7	Gold-Leaf	PVC film	Tattoo Paper	Vinyl Cutting	Yes	Slow	Gold-leaf needs larger electrode size and delicate to handle

Table 1. Results from exploration of material combinations. Recommended combinations are highlighted in bold font.
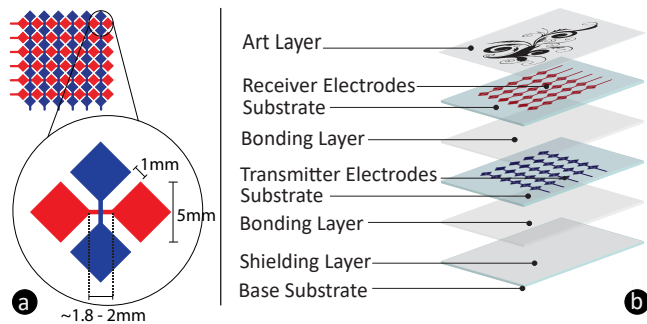

Figure 2. (a) Basic electrode design. (b) Layer-by-layer overview of the Multi-Touch Skin sensor.

Thus far, it has been unclear how to fabricate a mutual-capacitance based multi-touch touch sensor for use on skin, as the sensor needs to adapt to the mechanical, geometrical and electro-capacitive aspects of the body.

Since the Multi-Touch Skin sensor is very thin and worn directly on human skin, body capacitance effects of the user will manifest as parasitic noise in the sensor readings. These are hard to control for, as changing grounding conditions, skin conductivity, and internal body composition all affect the capacitive response of the body.

For robust functioning on the body, the sensor layout must be modified. This can be achieved by adding a shielding layer as the bottommost layer of the sensor [1, 14, 35, 48] (see Figure 2(b)). This layer acts as a fixed potential layer. It is fully covered with a conductor, and connected to the ground potential of the electrical circuitry. As demonstrated by empirical evaluation results presented in the evaluation section, this effectively masks body capacitive effects from the sensor measurements.

Hence, the main functional elements of the sensor film are three layers of conductors, patterned with electrodes and insulated by layers of dielectric material. Next, we identify suitable materials and fabrication techniques to realize them in a slim and flexible substrate.

Material Choices and Sensor Design

For our systematic exploration, we selected materials and fabrication techniques that have been successfully used in previous research on skin-based interfaces [52, 32, 24, 54].

Conductors: The most commonly used printable conductor is made of silver particles, which offer high conductivity at the cost of some brittleness. We used silver ink for ink-jet printing (Mitsubishi NBSIJ-MU01, $0.2\Omega/\square$ sheet resistance) and screen printing (Gwent C2131014D3, $0.1\Omega/\square$). A polymeric conductor (PEDOT-based translucent conductor, Gwent C2100629D1) offers better stretchability and translucency with a lower conductivity ($500-700k\Omega/\square$). Inspired by prior work, we also used aesthetic gold leaf and conductive carbon ink (Gwent C2130925D1, $15\Omega/\square$).

Dielectric: Prior work has reported successful use of printable dielectric paste (Gwent D2070209P6) and of the slimmer and transparent Resin Binder (Gwent R2070613P2). In addition, we tested simple PVC films ($\sim 7-15\mu m$ and $\sim 30-40\mu m$).

Base substrates: Temporary tattoo paper (Tattoo Decal Paper) is the slimmest material for printing used in prior work. In addition, we used transparent PET film for conductive ink-jet printing (Mitsubishi Paper Mill).

Fabrication technique: We investigated functional screen printing [42], as it is compatible with many printable materials. We tested conductive inkjet printing [25] with a commodity Canon IP100 desktop ink-jet printer, as it supports fast printing. Finally, we used vinyl cutting with gold leaf [24]. For sandwiching the layers and adhering the tattoo onto human skin, we used the adhesive that is supplied with the temporary rub-on tattoo paper.

Table 1 summarizes our observations on functional material combinations. We started by screen printing a full stack of functional layers on a single substrate, as proposed in prior work [42, 54]. However, it became apparent that these approaches either suffer from limited mechanical robustness due to a brittle dielectric paste that forms cracks on repeated deformations (#1,2), or insufficient conductivity of the PEDOT conductor for the mutual-capacitance controller chip (#3).

We therefore investigated an alternative fabrication approach. It uses a separate PVC film as the dielectric. The transmitting, receiving, and shielding electrode layers are each realized on a separate tattoo paper substrate, and then bonded to the dielectric film to create a multi-layer sandwich (illustrated in Figure 2(b)). For visual customization, the sensor can optionally be covered with a printed art layer. To ensure robust bonding of layers, we recommend to use 2-3 layers of tattoo paper adhesive, rather than just one. The electrode dimensions with exact spacing parameters are shown in Figure 2(a).

With this approach, we could realize functional sensors for use on skin, using all three basic fabrication techniques (approaches #4–7 in Table 1). Overall, we recommend using

approach #5 if a slim sensor design has a high priority, while #6 is the best approach when speed of fabrication is key. We used these approaches to realize all prototypes presented in this work.

High-fidelity printing
Screen printing is the preferred technique to realize a high-fidelity sensor that conforms to the user's skin, as it achieves very thin designs. We recommend to print silver overlaid with PEDOT:PSS (#5) to increase the robustness of the traces compared to silver only (#4). Prior work has shown this bridges the gaps when tiny cracks form in the silver conductor [54].

With our approach of printing the transmitter, receiver and shielding electrodes on separate substrates, we were able to realize multiple variations of Multi-Touch Skin sensors, which vary in their thickness and robustness. By choosing the dielectric PVC films of different thickness, the sensor can either be realized in a thinner form factor, which is more conformal to skin while being more delicate to handle; or it can be slightly thicker, and hence offer more mechanical robustness for rapid prototyping.

For our thinnest version, we used the tattoo paper substrate for the emitter, receiver, and shielding electrode layers. Between each pair of these layers, we sandwiched a PVC film of $\sim 30\mu m$ thickness as a dielectric and insulator. This results in an overall sensor thickness of $\sim 70 - 80\mu m$. An alternative version uses a thicker PET film of $\sim 70\mu m$ thickness, resulting in an overall thickness of $\sim 150 - 160\mu m$. The increase in thickness also eased sandwiching the layers.

Because thin gold leaf (approach #7) is delicate to handle and to manually apply onto the substrate, fabricating a sensor made of gold leaf takes longer and electrodes cannot be as small as with printed silver. This decreases the effective resolution. Prior work reported a minimum size of $\sim 1.4cm$ for electrodes made of gold leaves [24], whereas our printed silver electrodes measure 5mm. We therefore recommend this approach only if the aesthetics of the material is a key requirement.

Rapid fabrication using ink-jet printing
The Multi-Touch Skin sensor can be fabricated using a commodity ink-jet printer and silver ink (#6 in Table 1). This is by far the fastest technique, allowing to print all layers of the sensors in less than a minute. The sensor is also very robust, as the ink-jet-printable base substrate is thick (comparable to photo paper). However, this results in an overall sensor thickness of $\sim 400\mu m$.

Scalability
Mutual-capacitance sensing offers the advantage of easy scalability. We fabricated functional Multi-Touch Skin sensors with varying matrix dimensions (3×3, 4×4, 5×5, 6×3, 6×6, 10×6) that fit commonly used areas on the human body, such as the wrist and the forearm. Based on the touch-controller specification, we identified an electrode size of 5mm and a gap spacing of 1 mm between the receiver and transmitter electrodes (Figure 2(a)) to yield robust results [36]. A controlled evaluation reported below investigates scaling effects and demonstrates the high accuracy of multi-touch sensing.
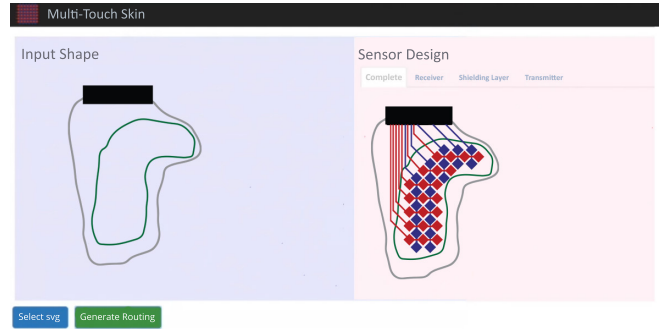

Figure 3. Screenshot of the design tool. (left) The designer specifies the touch-sensitive area S (green), the outer shape O of the full sensor sheet (gray) and the desired location of the connector C (black). (right) The tool generates the multi-touch sensor and provides the corresponding receiver, transmitter and shielding layers.

CUSTOMIZED FORM FACTORS
A multi-touch sensor for use on skin should be customizable to various sizes and (non-rectangular) shapes of the human body. This is not a trivial task for an interaction designer, since the intricate electrical parameters, such as electrode sizes, spacing, interconnections and distributions of the electrodes between layers, would need assistance from electrical engineering expertise. To the best of our knowledge, prior work has not yet addressed the question how to generate a multi-touch sensor layout for a given target shape. In this section, we introduce an approach for customizing the shape of mutual-capacitance touch sensors. We then present an interactive design tool that assists a designer in generating a functional sensor design for a desired custom shape.

Generating Custom-Shaped Multi-Touch Sensor Designs
Generating a multi-touch sensor design of a given 2D shape can be divided into two sub-tasks: first, the set of transmitter and receiver electrodes need to be generated to fit the shape; next, the interconnections between electrodes and an external connector should be generated.

Our method takes as input: 1. A polygon S defining the desired shape of the touch-sensitive area. 2. A polygon O defining the outer shape of the full sensor sheet (in addition to the touch-sensitive area, this includes additional space for routings and connector area). 3. The desired location of the connector area C in O, where a flexible flat cable will be attached for interfacing with the micro-controller (Figure 3 left).

The method is based on the fact that a minimum of two adjacent electrodes of different type (one transmitter TX and one receiver RX) are required for mutual-capacitance changes to be sensed. The algorithmic steps of the electrode generation process can be summarized as follows:

1. A rectangular bounding box S is generated and filled with a rectangular sensor matrix E, using the classical row-column diamond pattern of transmitter and receiver electrodes [27].

2. For each electrode e in E: If e is fully or partially outside of S, then it is removed.

3. Flag each remaining electrode e in E with a flag f for future inspection.

4. For each electrode e in E: If e has flag f, then

- For each neighbor electrode e' of e:

    - If e' has opposite type than e (TX vs. RX), then both e and e' are unflagged and move to next e in step 4.
    - If e' has same type as e (both RX or both TX), then move to next e'.

5. For each electrode e in E: If e has flag f, it is removed. This creates the final electrode set $\bar{E}$ (Figure 3 right).

Next, we use the A* algorithm [8] to series-connect the transmitting and receiving electrodes, to form lines and columns, and to wire them to the connector area. Routing of traces is restricted to the polygon O, to ensure the maximum sensor dimensions are not exceeded (Figure 3 right). If there is not enough space for routing on the polygon O, the method fails and marks those electrodes that could not be routed to; otherwise it returns the set of electrodes and the routings for the transmitting and receiving layers of the circuit.

Design Tool

To assist the designer in the sensor design process, we contribute a simple design tool that supports iterative design. It is implemented as a standalone web application using the JavaScript *svg.js* library[1] for reading and manipulating SVG files.

First, the designer uses a vector graphics application of choice to create an SVG file. It defines the desired contour of the sensor O, the shape of the functional sensor area S, and the connector placement C, using color-coded polygons. The tool reads this input file and implements the method described above. It outputs an SVG file that contains the print layout for all the printable layers.

We followed the *designer-in-the-loop* philosophy for our tool, in which the user can quickly inspect the outcome of the algorithm and if needed, slightly modify the shape. If the algorithm fails, it marks those electrodes in gray that did not fulfill the pre-conditions or that the A* algorithm could not route to. The designer can then iteratively modify the sensor shape (O, S and C) and re-run the algorithm until the result meets her expectations. The processing time of the algorithm to generate electrodes and routing varied between 3–8 secs for electrode numbers between $3\times3 - 10\times10$. Times were recorded on a portable computer (Intel Core i5).

We have successfully used our tool for generating various sensor designs of non-rectangular shape, including the functional prototypes of our application examples (see Figure 4). None of the sensors needed any calibration of the touch controller even though the lines have different electrical and capacitive characteristics. This is because mutual capacitance measures effects at the cross-section of two electrodes, and hence effects of wire length are less influential for the sizes on the body we are interested in and are normalized by the controller. Results
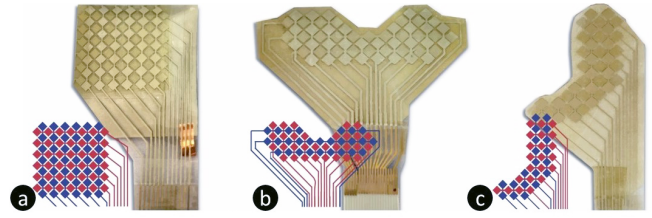
_____

Figure 4. Functional sensor prototypes of custom rectangular and non-rectangular shapes.

from our technical evaluation (see Figure 7) support this argument by showing less than 1mm change in location accuracy from 1×1 to 6×6 electrodes. This is below the human touch pointing accuracy reported in the literature (1.6mm [21]).

INTERFACING AND DATA PROCESSING

To enable the reader to replicate a functional sensor system, we now present the implementation details, including the electrical interfacing and data processing steps.

Electrical Interfacing and Data Capturing

The wearable controlling unit includes a Microchip MTCH6303 mutual capacitance multi-touch sensing chip with the MTCH652 transmit booster and a Raspberry Pi Zero. MTCH6303 is connected to the Raspberry through USB. The raw mutual capacitance values are read from the controller using the libUSB library at 100 Hz as an array of 10-bit unsigned data points representing each electrode cross-point. Data is then wirelessly transmitted to a desktop computer for further processing using a WebSocket through Wifi connection. The dimensions of the wearable controlling unit are $7 \times 4 \times 4$ cm (5(c). Its weight is ~ 60 grams.

Connections

Connecting flexible electronics with rigid circuitry, such as a controlling unit, is always a challenge. Previous work typically used copper tape and jumper wires for individual point-to-point connections [54]. While this solution works for smaller matrix sizes (e.g. 3×3), it is difficult to scale to larger ones because of the large number of individual wires. To realize a more scalable approach, we used thin and flexible flat cable (FFC) and connect it to the sensor with 3M conductive z-axis tape (see Figure 5)(c).

Data Processing Pipeline

We implemented a data processing pipeline to extract touch points and their properties (size, angle, etc.) from mutual capacitance data:

Step 1: Interpolation: Despite the relatively small number of electrodes, the sensor supports accurate spatial interpolation between cross-points. Microchip MTCH6303 senses capacitance changes for individual cross-point as continuous values spanning from 0 to 1024. By normalizing the capacitance and performing bi-linear interpolation, we create a 10*x* upscaled, interpolated capacitive image with continuous intensity values ranging from 0 to 1. For instance, for a sensor with 6×6 electrodes, the image has 60×60 pixels.

Step 2: Masking and Scaling: In order to remove noise, we mask the low intensity pixels of the image by setting pixels
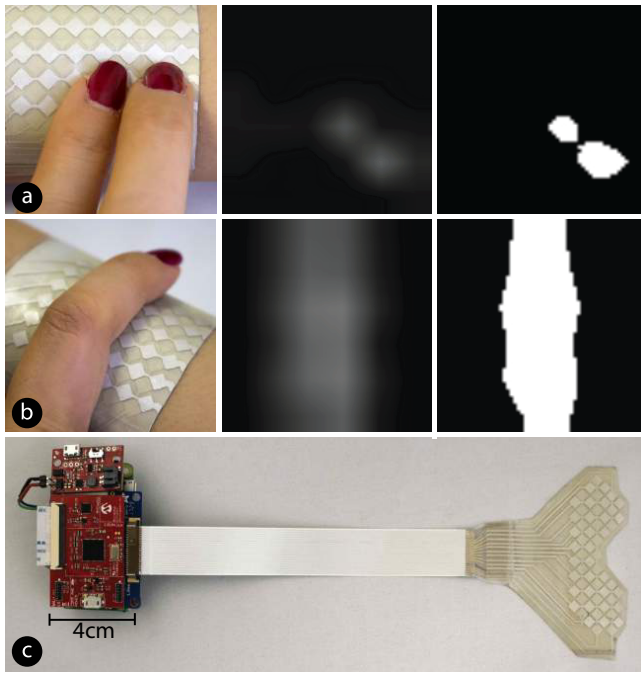
Figure 5. Detecting multi-touch input: a) minimum distance between two fingers which results in two distinct blobs, and the corresponding interpolated capacitive image and the extracted blobs; b) full finger placed on the sensor; c) the wearable hardware setup includes a Raspberry Pi Zero, the touch controller board and the Multi-Touch Skin Sensor.

with intensity less than 0.1 (10%) to 0. Then, the masked image's intensity values are linearly scaled, so that the maximum intensity is 1. This increases the contrast of the image, and highlights touch locations.

Step 3: Blob Extraction: The image is then subjected to thresholding to create a binary image. A pilot study showed that a threshold of (58%) to be the most appropriate. Connected white pixels in this binary image are grouped together to form blobs. Depending on the number of touch contacts, one or multiple blobs are extracted.

Figure 5(a and b) shows the results of the intermediate steps of the processing pipeline for several instances of touch input that were captured with a 6×6 sensor on the forearm.

EVALUATION

Three key aspects make Multi-Touch Skin different from conventional mutual-capacitance touch sensors: 1) The sensor is designed to be in constant contact with the body, 2) the sensor is deformable to fit different geometries on the body, and 3) the sensor needs to be scaled for different body locations. To formally evaluate the sensor's functionality with regard to these key differences, we conducted two controlled technical evaluations.

Study 1: Guarding Against Body Capacitance

Multi-Touch Skin is very thin and worn directly on the body. The body capacitance of a person can change rapidly and in an unpredictable way. Therefore, it must be investigated if the shielding layer can effectively guard sensor readings from such changes.
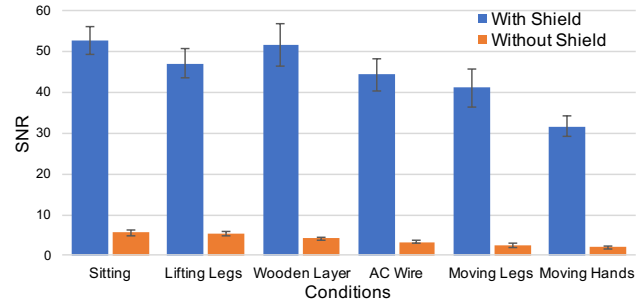

Figure 6. Signal-to-noise ratio of touch sensing on the body with and without the shielding layer.

Methodology

We collected mutual-capacitance data for 10 voluntary participants (avg. age : 26.9, SD = 2.1), with two sensor samples: one with the shielding layer (S1) and one without (S2). All other electrical and physical properties of S1 and S2 are kept the same. The sensors were consecutively placed at the exact same location on the non-dominant forearm of the participant. To test representative real-world situations, we collected touch data from each sensor in six different activity conditions that modified the grounding conditions, external electro-magnetic fields, and involved various types of physical movement: C1: sitting with forearm resting on table, and legs resting on floor; C2: same as C1 but lifting legs from the floor by $\sim$20 cm for 10 seconds; C3: same as C1 but with a wooden plank of 10 cm thickness between the feet and the floor: C4: same as C1 with touching the outside of an insulated active AC wire with the non-dominant hand; C5: standing on floor and walking at a fix location; C6: same as C1 with freely moving the non-dominant arm to the front and side of the torso. The order of all conditions and the sensors was counterbalanced.

For a given sensor and activity condition, the task consisted of repeatedly touching (5 trials) the sensor with the dominant hand's index finger for a $1s$ interval and releasing it for $1s$, as accurately as possible. Audio guidance for touch events was given by our study software. The participants were free to touch at any location on the sensor. The mutual capacitance values were recorded for all touch and no-touch conditions, and the signal-to-noise ratio (SNR) for touch events were calculated following the method presented in [7].

Results

Figure 6 shows the signal-to-noise ratio of the sensors with and without ground layer for the various activity conditions. In all conditions, the sensor with the shielding layer achieved a high signal-to-noise ratio (SNR), with average values ranging between 52.6 and 31.6. While the results show a decrease in SNR in case of body movement (C5 and C6) and external EM noise (C4), all values are considerably higher than 15, which is the minimum requirement for having robust touch sensing [7]. In contrast, the sensor without shielding layer had insufficient SNRs, ranging between 2.4 and 5. A two-way ANOVA confirmed a significant main effect of shielding ($p < 0.001$, $F = 639.1$). Overall, these results show that the shielding layer effectively shields the influence of body capacitance and ensures accurate functioning on the body.

Study 2: Flexibility and Scalability

Multi-Touch Skin will be deployed on different curvature conditions on the body and will need different scales to fit body locations. We set out to investigate how these conditions affect the spatial accuracy of touch input.

Methodology

We conducted a technical evaluation with three curvature conditions and three sensor sizes (3×3 factorial design) to evaluate the flexibility and scalability of the sensor. The curvature conditions are informed by the curvature of body locations that are commonly used for skin interfaces: fully flat state (C1); curved with a diameter of 45mm to reflect the typical curvature of a human wrist (C2); and curved with a diameter of 15mm to reflect the typical curvature of a human finger. The scalability conditions were chosen to reflect placement of the sensor on the finger tip (2×2 electrodes with 15×15 mm size), on the wrist (4×4 electrodes, 30×30 mm), and on the forearm (6×6 electrodes, 45×45 mm). The flat condition (C1) was chosen as the ground condition to comparatively assess potential detrimental effects of curvature.

Testing the sensor with the human body would have created multiple sources of strong bias that would have been impossible to control: First, prior work has shown that the human error of touch targeting is 1.6mm [21]. As this the expected accuracy of our sensor is higher, we would have studied human accuracy rather than the sensor's accuracy. Second, affixing the sensor on a natural body location would have made it impossible to control the curvature and angle of contact, because of continuous variations of curvature and underlying tissue at a given body location as well as involuntary body movements.

To ensure a controlled experiment setup and to be able to test the sensor's accuracy at a mm-scale, we therefore opted for a technical study. The sensor was affixed to a 3D printed flat (C1) or cylindrical object (C2 and C3), while touch input was performed with a conductive stylus (diameter $6mm$). We verified the capacitive signal generated by the stylus is similar in intensity to a typical touch contact of a human finger. To ensure precise and reproducible measurements, we laser cut stencils made of transparent acrylic (thickness 3mm) with holes on the target locations. Touch input was performed inside the holes with the stylus. The sensor was marked with visual markers for precisely aligning the stencil.

For each curvature condition, we measured the spatial accuracy on the sensor which reflect scale conditions 2×2, 4×4 and 6×6. We opted for locations which are farthest from the signal driving lines, because this is the location on the sensor that has the lowest spatial accuracy. For each scale $\times$ curvature condition, we tested three locations that were placed with $2mm$ distance. The locations are shown in Figure 7(b). At each of these locations, we captured three trials of two-second-long touch contact. Overall, this resulted in 3 (curvature conditions) $\times$ 3 (scale conditions) $\times$ 3 (locations) $\times$ 3 (trials) $\times$ 2 (seconds) $\times$ 100 (fps) = 16,200 data points for our analysis. For each sample, we calculated the distance between the actual location and the interpolated location that was calculated from capacitive sensor data.
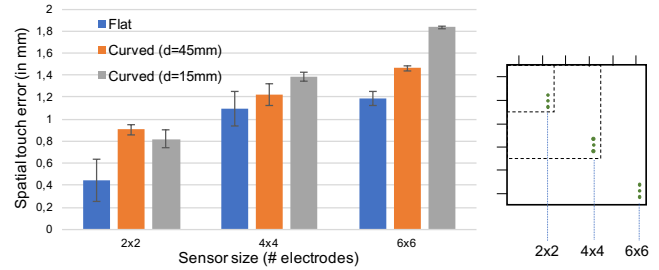

Figure 7. (a) Spatial accuracy of touch contact for different sensor sizes and curvatures. (b) The green dots show the locations on the sensor matrix which were used for evaluating the spatial accuracy.

Results

The results are depicted in Figure 7. An ANOVA identified a significant main effect of curvature ($p < 0.001$, $F = 15.53$) and of sensor size ($p < 0.001$, $F = 48.39$). Not surprisingly, accuracy is highest in the flat state (avg=0.91mm, SD=0.41) and lowest in the most deformed state (avg=1.35mm, SD=0.45). Likewise, accuracy decreases with increasing sensor sizes, averaging between 0.72mm (SD=0.28) for the 2×2 sensor and 1.49mm (SD=0.29) for the 6×6 sensor. The lowest accuracy we measured was 1.83mm, for the largest sensor in the most deformed state. This demonstrates that the sensors support high-resolution input in all curvature and scaling conditions. As shown in the Figure 7, the smallest sensor has a sub-millimeter accuracy in all deformation states. This implies it can be used for highly precise micro-gestures, e.g., when placed on the fingertip or on the finger's side.

To test whether these findings generalize to multi-touch input, we performed an additional small experiment. We compared the change in the reported locations of a touch contact when no other finger was touching the sensor and when another finger was touching the sensor on the same transmitter line or on the same receiver line. We did not see any significant change. This was expected, considering the sensor is using time-division multiplexing and sequentially measuring the mutual capacitance at each cross-section. Contrary to self-capacitance sensing, the effect of a second finger on mutual-capacitance is much lower and thus can be easily discarded in the filtering phase of processing. Minimum spacing between touch points is hard to formally evaluate (effects of angle, pressure etc.), but we can anecdotally report that the sensor detects two distinct blobs at a distance of $\sim 7mm$ between their centers (shown in Figure 5(a)).

APPLICATION EXAMPLES

To validate the fabrication approach for customized multi-touch sensor skins and to illustrate practical application scenarios, we have implemented four interactive application examples. These demonstrate the flexibility of the fabrication approach to realize various sensor sizes and shapes that are tailored for use on multiple body locations.

Multi-Touch Input on the Forearm

We realized a Multi-Touch Skin sensor with a 6×6 matrix of $45\times45mm$ size that can be worn on the forearm (Figure 1(a)). It is used for expressive gestural input for remote communication. Prior work has identified expressive ways of skin input

for remote communication [53]. The rich mutual-capacitance data of our sensor matrix now allows for the first time to detect such expressive gestures in a functional system. In addition to high-resolution single and multi-contact input, we can make use of the different blob signatures depending on the way the user touches the sensor. In our application, gestures are mapped to meaningful messages at the remote end. For instance, a grab gesture can be performed by covering the entire sensor with the hand to send a virtual hug to a loved one.

Multi-Touch EarStrap

Inspired from previous research on ear-based interfaces [31, 52], we fabricated a Multi-Touch Skin sensor in a non-rectangular form factor that fits behind the ear. The sensor features a 5×7 grid and has a tapered shape to match the body location (Figure 1(c)). Extending beyond prior work, it can detect continuous input along two dimensions and different types of touch contact: The user can swipe up or down to continuously set the volume. Swiping left and right switches between tracks. Placing the entire finger flat on the sensor can pause the music track.

One-Handed Input while Holding an Object

The bottom area of hand's inner side is a promising, yet under-explored area for body-based interaction. It is accessible for multiple fingers, even while holding a thin object, such as a bag's handle or a pen. We realized a non-rectangular Multi-Touch Skin sensor for this body location, designed such that it does not occlude the palm's area. It features a 10×6 matrix with $101\times65mm$ in size (Figure 1(d)). In our application, the user can easily accept or reject calls when the hand is occupied, by tapping with one or two fingers on the sensor. This extends the set of interactions for palm-based input [9, 51, 15].

Multi-Touch Bracelet

Previous research realizes touch buttons and single-touch sliders on a watch strap [43]. We improve by realizing a Multi-Touch Skin sensor for the wrist. The sensor features a 8×3 matrix and is $77\times25mm$ in size (Fig. 1(b)). In our application, the user to controls a smart lamp (Philips Hue), interfaced via wifi. The user can place two fingers around the wrist and rotate to change the color of a light bulb. Swiping alongside the bracelet with two fingers controls the brightness of the lamp. Using two contacts instead of only one reduces the likelihood of false activation.

LIMITATIONS AND FUTURE WORK

Extreme deformations: The evaluation results showed that the sensor accurately captures touch input despite strong curvature, as it occurs for example on the finger. If worn on a joint, such as the wrist, local maxima of curvature can extend beyond this. It remains to be formally investigated to what extent the sensor can withstand such strong and repeated deformations, and if the functionality is affected. Anecdotally we can report that we tested the sensor when placed on the wrist. Despite strong bending, which created a fold on the sensor, it correctly detected touch input at all areas, except on the fold itself. The fold showed a unique capacitive signature, which lets us believe that future generations of sensors might be able detect their deformation.

Scalability: We have formally evaluated sensor scalability up to a size of 6×6. This reflects a typical size on many body locations. We have also realized a functional 10×6 sensor prototype. This is hinting at a higher scalability, but needs to be formally evaluated. Technically, the controller we used can support up to 27×18 electrodes. An important limitation of all today's skin electronics is the connection between the flexible sensor and the rigid controller. This provides a practical barrier to upscaling to significantly larger sizes. With the FFC-based connector, we have presented a novel solution that makes it easier for the HCI community to connect larger sensors.

Design tool: The design tool is limited in that it only considers full electrodes. Future versions could also consider placing partial electrodes or having non-uniform electrode sizes to more closely match the desired sensor's shape. Moreover, they could optimize the shape of the sensor and the controller placement to realize a high-quality result without design iterations. Moreover, future implementations could realize the tool as a plug-in for a vector graphics application, or even include body scanning [39], to ease design and iterative refinement.

Extended Usage: Our preliminary observations show that Multi-Touch Skin is robust and is functional over multiple days. This is supported by the fact that for study 1, we used the same sensor sample for all users; furthermore, in an informal study, three users wore the sensor on the forearm for half a work day (4-6 h) in an office setting. At the end of the experiment, we also gathered feedback on the ergonomics of the sensor. The user feedback was positive in general, highlighting the minimal invasiveness of Multi-Touch Skin. For instance, one of the participants stated: "The sensor is really thin, fits on to the skin and I cannot feel it doing my everyday tasks (P1)". These anecdotal findings show the potential of Multi-Touch Skin for using it on a daily basis. However, a more extensive "in-the-wild" investigation is required to properly understand the usability and functionality of the sensor under extended physical activities.

CONCLUSION

We have presented the first method that allows interaction designers to design and fabricate functional and high-resolution multi-touch sensor skins for the body. This includes a design tool that assists the designer in generating sensors of custom and non-rectangular shape, and the first technique for printing a mutual-capacitance sensor on a commodity inkjet printer. A set of functional sensors and practical application examples, as well as results from two technical studies demonstrate the sensor's functionality on the human body, in various scales, and when undergoing significant deformation. Promising avenues for future work comprise advanced design tools for the body and simultaneous sensing of multiple modalities.

REFERENCES

1. A Arogbonlo, C Usma, AZ Kouzani, and I Gibson. 2015. Design and Fabrication of a Capacitance Based Wearable Pressure Sensor Using E-textiles. *Procedia Technology* 20 (2015), 270–275.

2. Daniel Ashbrook, Patrick Baudisch, and Sean White. 2011. Nenya: Subtle and Eyes-free Mobile Input with a Magnetically-tracked Finger Ring. In *Proceedings of the SIGCHI Conference on Human Factors in Computing Systems (CHI '11)*. ACM, New York, NY, USA, 2043–2046. DOI: http://dx.doi.org/10.1145/1978942.1979238

3. Gary Barrett and Ryomei Omote. 2010. Projected-capacitive touch technology. *Information Display* 26, 3 (2010), 16–21.

4. Frank Beck and Bent Stumpe. 1973. *Two devices for operator interaction in the central control of the new CERN accelerator*. Technical Report. CERN.

5. Liwei Chan, Yi-Ling Chen, Chi-Hao Hsieh, Rong-Hao Liang, and Bing-Yu Chen. 2015. CyclopsRing: Enabling Whole-Hand and Context-Aware Interactions Through a Fisheye Ring. In *Proceedings of the 28th Annual ACM Symposium on User Interface Software & Technology (UIST '15)*. ACM, New York, NY, USA, 549–556. DOI: http://dx.doi.org/10.1145/2807442.2807450

6. Liwei Chan, Rong-Hao Liang, Ming-Chang Tsai, Kai-Yin Cheng, Chao-Huai Su, Mike Y. Chen, Wen-Huang Cheng, and Bing-Yu Chen. 2013. FingerPad: Private and Subtle Interaction Using Fingertips. In *Proceedings of the 26th Annual ACM Symposium on User Interface Software and Technology (UIST '13)*. ACM, New York, NY, USA, 255–260. DOI: http://dx.doi.org/10.1145/2501988.2502016

7. Burke Davison. 2010. Techniques for robust touch sensing design. *AN1334 Microchip Technology Inc* (2010), 53.

8. Daniel Delling, Peter Sanders, Dominik Schultes, and Dorothea Wagner. 2009. *Engineering Route Planning Algorithms*. Springer Berlin Heidelberg, Berlin, Heidelberg, 117–139. DOI: http://dx.doi.org/10.1007/978-3-642-02094-0_7

9. Niloofar Dezfuli, Mohammadreza Khalilbeigi, Jochen Huber, Florian Müller, and Max Mühlhäuser. 2012. PalmRC: Imaginary Palm-based Remote Control for Eyes-free Television Interaction. In *Proceedings of the 10th European Conference on Interactive Tv and Video (EuroiTV '12)*. ACM, New York, NY, USA, 27–34. DOI: http://dx.doi.org/10.1145/2325616.2325623

10. Paul Dietz and Darren Leigh. 2001. DiamondTouch: A Multi-user Touch Technology. In *Proceedings of the 14th Annual ACM Symposium on User Interface Software and Technology (UIST '01)*. ACM, New York, NY, USA, 219–226. DOI:http://dx.doi.org/10.1145/502348.502389

11. David Dobbelstein, Christian Winkler, Gabriel Haas, and Enrico Rukzio. 2017. PocketThumb: a Wearable Dual-Sided Touch Interface for Cursor-based Control of Smart-Eyewear. *Proceedings of the ACM on Interactive, Mobile, Wearable and Ubiquitous Technologies* 1, 2 (2017), 9.

12. Nan-Wei Gong, Jürgen Steimle, Simon Olberding, Steve Hodges, Nicholas Edward Gillian, Yoshihiro Kawahara, and Joseph A Paradiso. 2014. PrintSense: a versatile sensing technique to support multimodal flexible surface interaction. In *Proceedings of the 32nd annual ACM conference on Human factors in computing systems*. ACM, 1407–1410.

13. Tobias Grosse-Puppendahl, Christian Holz, Gabe Cohn, Raphael Wimmer, Oskar Bechtold, Steve Hodges, Matthew S. Reynolds, and Joshua R. Smith. 2017. Finding Common Ground: A Survey of Capacitive Sensing in Human-Computer Interaction. In *Proceedings of the SIGCHI Conference on Human Factors in Computing Systems (CHI '17)*. ACM, New York, NY, USA. DOI:http://dx.doi.org/10.1145/3025453.3025808

14. Xiaohui Guo, Ying Huang, Xia Cai, Caixia Liu, and Ping Liu. 2016. Capacitive wearable tactile sensor based on smart textile substrate with carbon black/silicone rubber composite dielectric. *Measurement Science and Technology* 27, 4 (2016), 045105.

15. Sean Gustafson, Christian Holz, and Patrick Baudisch. 2011. Imaginary phone: learning imaginary interfaces by transferring spatial memory from a familiar device. In *Proceedings of the 24th annual ACM symposium on User interface software and technology*. ACM, 283–292.

16. Sean G. Gustafson, Bernhard Rabe, and Patrick M. Baudisch. 2013. Understanding palm-based imaginary interfaces. In *Proceedings of the SIGCHI Conference on Human Factors in Computing Systems - CHI '13*. ACM Press, New York, New York, USA, 889. DOI: http://dx.doi.org/10.1145/2470654.2466114

17. Chris Harrison, Hrvoje Benko, and Andrew D. Wilson. 2011. OmniTouch: Wearable Multitouch Interaction Everywhere. In *Proceedings of the 24th Annual ACM Symposium on User Interface Software and Technology (UIST '11)*. ACM, New York, NY, USA, 441–450. DOI: http://dx.doi.org/10.1145/2047196.2047255

18. Chris Harrison and Scott E. Hudson. 2009. Abracadabra: Wireless, High-precision, and Unpowered Finger Input for Very Small Mobile Devices. In *Proceedings of the 22Nd Annual ACM Symposium on User Interface Software and Technology (UIST '09)*. ACM, New York, NY, USA, 121–124. DOI: http://dx.doi.org/10.1145/1622176.1622199

19. Chris Harrison, Desney Tan, and Dan Morris. 2010. Skinput: Appropriating the Body As an Input Surface. In *Proceedings of the SIGCHI Conference on Human Factors in Computing Systems (CHI '10)*. ACM, New York, NY, USA, 453–462. DOI: http://dx.doi.org/10.1145/1753326.1753394

20. Florian Heller, Stefan Ivanov, Chat Wacharamanotham, and Jan Borchers. 2014. FabriTouch: Exploring Flexible Touch Input on Textiles. In *Proceedings of the 2014 ACM International Symposium on Wearable Computers (ISWC '14)*. ACM, New York, NY, USA, 59–62. `DOI:` `http://dx.doi.org/10.1145/2634317.2634345`

21. Christian Holz and Patrick Baudisch. 2011. Understanding touch. In *Proceedings of the SIGCHI Conference on Human Factors in Computing Systems*. ACM, 2501–2510.

22. Da-Yuan Huang, Liwei Chan, Shuo Yang, Fan Wang, Rong-Hao Liang, De-Nian Yang, Yi-Ping Hung, and Bing-Yu Chen. 2016. DigitSpace: Designing Thumb-to-Fingers Touch Interfaces for One-Handed and Eyes-Free Interactions. In *Proceedings of the 2016 CHI Conference on Human Factors in Computing Systems (CHI '16)*. ACM, New York, NY, USA, 1526–1537. `DOI:` `http://dx.doi.org/10.1145/2858036.2858483`

23. Hsin-Liu (Cindy) Kao, Artem Dementyev, Joseph A. Paradiso, and Chris Schmandt. 2015. NailO: Fingernails As an Input Surface. In *Proceedings of the 33rd Annual ACM Conference on Human Factors in Computing Systems (CHI '15)*. ACM, New York, NY, USA, 3015–3018. `DOI:` `http://dx.doi.org/10.1145/2702123.2702572`

24. Hsin-Liu (Cindy) Kao, Christian Holz, Asta Roseway, Andres Calvo, and Chris Schmandt. 2016. DuoSkin: Rapidly Prototyping On-skin User Interfaces Using Skin-friendly Materials. In *Proceedings of the 2016 ACM International Symposium on Wearable Computers (ISWC '16)*. ACM, New York, NY, USA, 16–23. `DOI:` `http://dx.doi.org/10.1145/2971763.2971777`

25. Yoshihiro Kawahara, Steve Hodges, Benjamin S Cook, Cheng Zhang, and Gregory D Abowd. 2013. Instant inkjet circuits: lab-based inkjet printing to support rapid prototyping of UbiComp devices. In *Proceedings of the 2013 ACM international joint conference on Pervasive and ubiquitous computing*. ACM, 363–372.

26. Gierad Laput, Robert Xiao, Xiang 'Anthony' Chen, Scott E. Hudson, and Chris Harrison. 2014. Skin Buttons: Cheap, Small, Low-powered and Clickable Fixed-icon Laser Projectors. In *Proceedings of the 27th Annual ACM Symposium on User Interface Software and Technology (UIST '14)*. ACM, New York, NY, USA, 389–394. `DOI:` `http://dx.doi.org/10.1145/2642918.2647356`

27. J. Lee, M. T. Cole, J. C. S. Lai, and A. Nathan. 2014. An Analysis of Electrode Patterns in Capacitive Touch Screen Panels. *Journal of Display Technology* 10, 5 (May 2014), 362–366. `DOI:` `http://dx.doi.org/10.1109/JDT.2014.2303980`

28. SK Lee, William Buxton, and K. C. Smith. 1985. A Multi-touch Three Dimensional Touch-sensitive Tablet. In *Proceedings of the SIGCHI Conference on Human Factors in Computing Systems (CHI '85)*. ACM, New York, NY, USA, 21–25. `DOI:` `http://dx.doi.org/10.1145/317456.317461`

29. Rong-Hao Liang, Shu-Yang Lin, Chao-Huai Su, Kai-Yin Cheng, Bing-Yu Chen, and De-Nian Yang. 2011. SonarWatch: Appropriating the Forearm As a Slider Bar. In *SIGGRAPH Asia 2011 Emerging Technologies (SA '11)*. ACM, New York, NY, USA, Article 5, 1 pages. `DOI:` `http://dx.doi.org/10.1145/2073370.2073374`

30. Jaime Lien, Nicholas Gillian, M. Emre Karagozler, Patrick Amihood, Carsten Schwesig, Erik Olson, Hakim Raja, and Ivan Poupyrev. 2016. Soli: Ubiquitous Gesture Sensing with Millimeter Wave Radar. *ACM Trans. Graph.* 35, 4, Article 142 (July 2016), 19 pages. `DOI:` `http://dx.doi.org/10.1145/2897824.2925953`

31. Roman Lissermann, Jochen Huber, Aristotelis Hadjakos, and Max Mühlhäuser. 2013. EarPut: Augmenting Behind-the-ear Devices for Ear-based Interaction. In *CHI '13 Extended Abstracts on Human Factors in Computing Systems (CHI EA '13)*. ACM, New York, NY, USA, 1323–1328. `DOI:` `http://dx.doi.org/10.1145/2468356.2468592`

32. Joanne Lo, Doris Jung Lin Lee, Nathan Wong, David Bui, and Eric Paulos. 2016. Skintillates: Designing and Creating Epidermal Interactions. In *Proceedings of the 2016 ACM Conference on Designing Interactive Systems (DIS '16)*. ACM, New York, NY, USA, 853–864. `DOI:` `http://dx.doi.org/10.1145/2901790.2901885`

33. Siyuan Ma, Flavio Ribeiro, Karlton Powell, John Lutian, Christian Møller, Timothy Large, and James Holbery. 2015. Fabrication of novel transparent touch sensing device via drop-on-demand inkjet printing technique. *ACS applied materials & interfaces* 7, 39 (2015), 21628–21633.

34. Denys J. C. Matthies, Simon T. Perrault, Bodo Urban, and Shengdong Zhao. 2015. Botential: Localizing On-Body Gestures by Measuring Electrical Signatures on the Human Skin. In *Proceedings of the 17th International Conference on Human-Computer Interaction with Mobile Devices and Services (MobileHCI '15)*. ACM, New York, NY, USA, 207–216. `DOI:` `http://dx.doi.org/10.1145/2785830.2785859`

35. Jan Meyer, Bert Arnrich, Johannes Schumm, and Gerhard Troster. 2010. Design and modeling of a textile pressure sensor for sitting posture classification. *IEEE Sensors Journal* 10, 8 (2010), 1391–1398.

36. Microchip. MTCH6301 Touch Controller Datasheet. `http://ww1.microchip.com/downloads/en/DeviceDoc/` `40001663B.pdf`. (????). Accessed: 2017-12-24.

37. Adiyan Mujibiya, Xiang Cao, Desney S. Tan, Dan Morris, Shwetak N. Patel, and Jun Rekimoto. 2013. The Sound of Touch: On-body Touch and Gesture Sensing Based on Transdermal Ultrasound Propagation. In *Proceedings of the 2013 ACM International Conference on Interactive Tabletops and Surfaces (ITS '13)*. ACM, New York, NY, USA, 189–198. `DOI:` `http://dx.doi.org/10.1145/2512349.2512821`

38. Kei Nakatsuma, Hiroyuki Shinoda, Yasutoshi Makino, Katsunari Sato, and Takashi Maeno. 2011. Touch Interface on Back of the Hand. In *ACM SIGGRAPH 2011 Posters (SIGGRAPH '11)*. ACM, New York, NY, USA, Article 39, 1 pages. DOI:
http://dx.doi.org/10.1145/2037715.2037760

39. Aditya Shekhar Nittala and Jürgen Steimle. 2016. Digital fabrication pipeline for on-body sensors: design goals and challenges. In *Proceedings of the 2016 ACM International Joint Conference on Pervasive and Ubiquitous Computing: Adjunct*. ACM, 950–953.

40. Masa Ogata, Yuta Sugiura, Yasutoshi Makino, Masahiko Inami, and Michita Imai. 2013. SenSkin: Adapting Skin As a Soft Interface. In *Proceedings of the 26th Annual ACM Symposium on User Interface Software and Technology (UIST '13)*. ACM, New York, NY, USA, 539–544. DOI:
http://dx.doi.org/10.1145/2501988.2502039

41. Simon Olberding, Nan-Wei Gong, John Tiab, Joseph A Paradiso, and Jürgen Steimle. 2013. A cuttable multi-touch sensor. In *Proceedings of the 26th annual ACM symposium on User interface software and technology*. ACM, 245–254.

42. Simon Olberding, Michael Wessely, and Jürgen Steimle. 2014. PrintScreen: Fabricating Highly Customizable Thin-film Touch-displays. In *Proceedings of the 27th Annual ACM Symposium on User Interface Software and Technology (UIST '14)*. ACM, New York, NY, USA, 281–290. DOI:
http://dx.doi.org/10.1145/2642918.2647413

43. Simon T Perrault, Eric Lecolinet, James Eagan, and Yves Guiard. 2013. Watchit: simple gestures and eyes-free interaction for wristwatches and bracelets. In *Proceedings of the SIGCHI Conference on Human Factors in Computing Systems*. ACM, 1451–1460.

44. Ivan Poupyrev, Nan-Wei Gong, Shiho Fukuhara, Mustafa Emre Karagozler, Carsten Schwesig, and Karen E. Robinson. 2016. Project Jacquard: Interactive Digital Textiles at Scale. In *Proceedings of the 2016 CHI Conference on Human Factors in Computing Systems (CHI '16)*. ACM, New York, NY, USA, 4216–4227. DOI:
http://dx.doi.org/10.1145/2858036.2858176

45. Ivan Poupyrev, Philipp Schoessler, Jonas Loh, and Munehiko Sato. 2012. Botanicus Interacticus: Interactive Plants Technology. In *ACM SIGGRAPH 2012 Emerging Technologies (SIGGRAPH '12)*. ACM, New York, NY, USA, Article 4, 1 pages. DOI:
http://dx.doi.org/10.1145/2343456.2343460

46. Jun Rekimoto. 2002. SmartSkin: An Infrastructure for Freehand Manipulation on Interactive Surfaces. In *Proceedings of the SIGCHI Conference on Human Factors in Computing Systems (CHI '02)*. ACM, New York, NY, USA, 113–120. DOI:
http://dx.doi.org/10.1145/503376.503397

47. Munehiko Sato, Ivan Poupyrev, and Chris Harrison. 2012. Touché: Enhancing Touch Interaction on Humans, Screens, Liquids, and Everyday Objects. In *Proceedings of the SIGCHI Conference on Human Factors in Computing Systems (CHI '12)*. ACM, New York, NY, USA, 483–492. DOI:
http://dx.doi.org/10.1145/2207676.2207743

48. Gurashish Singh, Alexander Nelson, Ryan Robucci, Chintan Patel, and Nilanjan Banerjee. 2015. Inviz: Low-power personalized gesture recognition using wearable textile capacitive sensor arrays. In *Pervasive Computing and Communications (PerCom), 2015 IEEE International Conference on*. IEEE, 198–206.

49. Hyunyoung Song, Hrvoje Benko, Francois Guimbretiere, Shahram Izadi, Xiang Cao, and Ken Hinckley. 2011. Grips and Gestures on a Multi-touch Pen. In *Proceedings of the SIGCHI Conference on Human Factors in Computing Systems (CHI '11)*. ACM, New York, NY, USA, 1323–1332. DOI:
http://dx.doi.org/10.1145/1978942.1979138

50. Jürgen Steimle, Joanna Bergstrom-Lehtovirta, Martin Weigel, Aditya Shekhar Nittala, Sebastian Boring, Alex Olwal, and Kasper Hornbæk. 2017. On-Skin Interaction Using Body Landmarks. *Computer* 50, 10 (2017), 19–27.

51. Cheng-Yao Wang, Wei-Chen Chu, Po-Tsung Chiu, Min-Chieh Hsiu, Yih-Harn Chiang, and Mike Y. Chen. 2015. PalmType: Using Palms As Keyboards for Smart Glasses. In *Proceedings of the 17th International Conference on Human-Computer Interaction with Mobile Devices and Services (MobileHCI '15)*. ACM, New York, NY, USA, 153–160. DOI:
http://dx.doi.org/10.1145/2785830.2785886

52. Martin Weigel, Tong Lu, Gilles Bailly, Antti Oulasvirta, Carmel Majidi, and Jürgen Steimle. 2015. iSkin: Flexible, Stretchable and Visually Customizable On-Body Touch Sensors for Mobile Computing. In *Proceedings of the 33rd Annual ACM Conference on Human Factors in Computing Systems (CHI '15)*. ACM, New York, NY, USA, 2991–3000. DOI:
http://dx.doi.org/10.1145/2702123.2702391

53. Martin Weigel, Vikram Mehta, and Jürgen Steimle. 2014. More Than Touch: Understanding How People Use Skin As an Input Surface for Mobile Computing. In *Proceedings of the SIGCHI Conference on Human Factors in Computing Systems (CHI '14)*. ACM, New York, NY, USA, 179–188. DOI:
http://dx.doi.org/10.1145/2556288.2557239

54. Martin Weigel, Aditya Shekhar Nittala, Alex Olwal, and Jürgen Steimle. 2017. SkinMarks : Enabling Interaction on Body Landmarks Using Conformal Skin Electronics. In *Proceedings of the SIGCHI Conference on Human Factors in Computing Systems (CHI '17)*. ACM, New York, NY, USA. DOI:
http://dx.doi.org/10.1145/3025453.3025704

55. Yang Zhang, Junhan Zhou, Gierad Laput, and Chris Harrison. 2016. SkinTrack: Using the Body As an Electrical Waveguide for Continuous Finger Tracking on the Skin. In *Proceedings of the 2016 CHI Conference on Human Factors in Computing Systems (CHI '16)*. ACM, New York, NY, USA, 1491–1503. `DOI:` `http://dx.doi.org/10.1145/2858036.2858082`

56. Junhan Zhou, Yang Zhang, Gierad Laput, and Chris Harrison. 2016. AuraSense: Enabling Expressive Around-Smartwatch Interactions with Electric Field Sensing. In *Proceedings of the 29th Annual Symposium on User Interface Software and Technology (UIST '16)*. ACM, New York, NY, USA, 81–86. `DOI:` `http://dx.doi.org/10.1145/2984511.2984568`

57. Thomas G Zimmerman, Joshua R Smith, Joseph A Paradiso, David Allport, and Neil Gershenfeld. 1995. Applying electric field sensing to human-computer interfaces. In *Proceedings of the SIGCHI conference on Human factors in computing systems*. ACM Press/Addison-Wesley Publishing Co., 280–287.